

NKG2D Controls Natural Reactivity of V γ 9V δ 2 T Lymphocytes against Mesenchymal Glioblastoma Cells



Cynthia Chauvin^{1,2}, Noémie Joalland^{1,2}, Jeanne Perroteau^{1,2}, Ulrich Jarry^{1,2}, Laura Lafrance^{1,2}, Catherine Willem^{1,3}, Christelle Retière^{1,3}, Lisa Oliver^{1,4}, Catherine Gratas^{1,4}, Laetitia Gautreau-Rolland^{1,2}, Xavier Saulquin^{1,2}, François M. Vallette^{1,2,5}, Henri Vié^{1,2}, Emmanuel Scotet^{1,2}, and Claire Pecqueur^{1,2}

Abstract

Purpose: Cellular immunotherapies are currently being explored to eliminate highly invasive and chemoradioresistant glioblastoma (GBM) cells involved in rapid relapse. We recently showed that concomitant stereotactic injections of non-alloreactive allogeneic V γ 9V δ 2 T lymphocytes eradicate zoledronate-primed human GBM cells. In the present study, we investigated the spontaneous reactivity of allogeneic human V γ 9V δ 2 T lymphocytes toward primary human GBM cells, *in vitro* and *in vivo*, in the absence of any prior sensitization.

Experimental Design: Through functional and transcriptomic analyses, we extensively characterized the immunoreactivity of human V γ 9V δ 2 T lymphocytes against various primary GBM cultures directly derived from patient tumors.

Results: We evidenced that GBM cells displaying a mesenchymal signature are spontaneously eliminated by allogeneic human V γ 9V δ 2 T lymphocytes, a reactivity process being mediated by $\gamma\delta$ T-cell receptor (TCR) and tightly regulated by cellular stress-associated NKG2D pathway. This led to the identification of highly reactive V γ 9V δ 2 T lymphocyte populations, independently of a specific TCR repertoire signature. Moreover, we finally provide evidence of immunotherapeutic efficacy *in vivo*, in the absence of any prior tumor cell sensitization.

Conclusions: By identifying pathways implicated in the selective natural recognition of mesenchymal GBM cell subtypes, accounting for 30% of primary diagnosed and 60% of recurrent GBM, our results pave the way for novel targeted cellular immunotherapies.

Introduction

Glioblastomas (GBMs) are the most frequent primary brain tumors in adult with an incidence of five per 100,000 people.

¹CRCINA, INSERM, CNRS, Université d'Angers, Université de Nantes, Nantes, France. ²LabEx IGO "Immunotherapy, Graft, Oncology," Nantes, France. ³Etablissement Français du Sang, Nantes, France. ⁴Centre Hospitalier-Universitaire (CHU) de Nantes, Nantes, France. ⁵Institut de Cancérologie de l'Ouest (ICO), St Herblain, France.

Note: Supplementary data for this article are available at Clinical Cancer Research Online (<http://clincancerres.aacrjournals.org/>).

C. Chauvin and N. Joalland contributed equally to this article.

E. Scotet and C. Pecqueur contributed equally to this article.

Corresponding Authors: Claire Pecqueur, CRCINA, INSERM, CNRS, Université d'Angers, Université de Nantes, 8 quai Moncousu, 44007 Nantes, France. Phone: 332-0228-080302; Fax: 332-0228-080204; E-mail: claire.pecqueur@univ-nantes.fr; and Emmanuel Scotet, Centre de Recherche en Cancérologie et Immunologie Nantes-Angers, INSERM UMR1232 CNRS ERL6001, Université de Nantes, 8 quai Moncousu, 44007 Nantes, France. Phone: 33-2-2808-0222; Fax: 332-2808-0204; E-mail: emmanuel.scotet@univ-nantes.fr

Clin Cancer Res 2019;25:7218–28

doi: 10.1158/1078-0432.CCR-19-0375

©2019 American Association for Cancer Research.

Current standard therapy, defined by the Stupp protocol, includes surgery followed by radiotherapy with concomitant and adjuvant chemotherapy (1). Despite such aggressive treatments, the median survival does not exceed 18 months, with less than 5% of patients alive at 5 years. This dismal prognosis might be explained by deep invasive tumor growth, limited surgical efficiency, poor drug delivery across the blood–brain barrier, and a high degree of GBM tumor heterogeneity. First, GBM display intertumor heterogeneity mostly characterized by distinct genetic alterations occurring in individual tumors and leading to various responses in patients. The genetic landscape of GBM has been performed through genome-wide association studies allowing the identification of up to four molecular subtypes with relative prognostic or predictive significance (2, 3). There are marked differences between the mesenchymal subtype (MES) and the three others (defined here as CNP, referring to Classical, Neural, and Proneural subtypes). The MES subtype is associated with poor survival, in contrast to CNP subtype which is generally associated with a more favorable outcome (2, 4, 5). Second, spatial heterogeneity within the same tumor, including active tumor zones as well as hypoxic and necrotic zones, is common in GBM (6, 7). Importantly, hypoxic zones constitute cellular niches for MES GBM cells and also cancer stem-like cells (CSCs) with singular phenotypic properties including transient quiescence, self-renewal, resistance to radiation-induced DNA damages, and the ability to reconstitute the initial tumor. Thus, new strategies targeting highly

Translational Relevance

Glioblastoma (GBM) representing the majority of primary malignant brain tumors displays a dismal prognosis with a recurrence rate of more than 90%. Therapeutic immunotherapies, including the emerging use of adoptive cell therapy, have shown promising antitumor efficacy. In this work, we clearly show that the more resistant subsets of GBM cells are spontaneously killed by nonalloreactive allogeneic human V γ 9V δ 2 T-lymphocyte effectors. This natural reactivity process, mediated by the $\gamma\delta$ T-cell receptor and tightly regulated by cellular stress-associated NKG2D pathway, led to the identification of highly reactive allogeneic V γ 9V δ 2 T-lymphocyte subsets. Importantly, we provide evidence of allogeneic V γ 9V δ 2 T-lymphocyte immunotherapy efficacy *in vivo*, in the absence of any prior tumor cell sensitization. Our study brings new insights into novel immunotherapeutic options for therapy directed at the recurrence of GBM based on adoptive transfer of allogeneic V γ 9V δ 2 T lymphocytes at the tumor bed.

resistant cancer cells, including mesenchymal GBM cells and CSC, may significantly improve patients' outcomes.

In line with their spectacular effects evidenced in various solid and circulating cancer indications (8–11), immunotherapies have also been proposed for treating patients with GBM (12), including adoptive transfer of immune cells. Among attractive immune effectors, peripheral V γ 9V δ 2 T lymphocytes, mostly present in primates and representing 5% to 10% of blood CD3⁺ lymphocytes in healthy adults, are important players in natural host defenses against infection and malignancies (13). These transitional T lymphocytes are selectively activated in a T-cell receptor (TCR)-dependent, but MHC-independent, manner, by nonpeptidic small molecules [hereafter called phosphoantigens (PAG)], such as isopenentenyl pyrophosphate. Accordingly, target cells' sensitization by pharmacologic aminobisphosphonate (NBP) compounds, such as zoledronate, inhibits a key enzyme of the mammalian mevalonate pathway that degrades PAG and upregulates the reactivity of V γ 9V δ 2 T lymphocytes. We have described a mandatory role played by BTN3A/CD277 butyrophilins which are type I glycoproteins from the B7 superfamily in this still unclear reactivity process (14–16). Besides TCR-dependent mechanism, cell recognition and subsequent V γ 9V δ 2 T-lymphocyte activation also involve the engagement of natural killer (NK) receptors, such as the activating NKG2D (*natural killer group 2, member D*) receptor (17). This receptor recognizes stress-induced molecular determinants that are barely expressed by healthy cells while often upregulated by infected or transformed cells. Importantly, given the absence of MHC restriction, the injection of allogeneic V γ 9V δ 2 T lymphocytes within the surrounding cerebral parenchyma following tumor resection represents a unique opportunity to deliver elevated quantities of tumor-reactive T lymphocytes in the vicinity of residual malignancy. In line with this, we showed that concomitant stereotactic injections of allogeneic V γ 9V δ 2 T lymphocytes and zoledronate eradicate human GBM cells *in vivo* (18). This study also showed that V γ 9V δ 2 T lymphocytes display unexpected efficient and natural cytotoxicity against some human GBM cells (19).

In the present study, we investigated the molecular mechanisms regulating the spontaneous reactivity of allogeneic human

V γ 9V δ 2 T lymphocytes toward some human GBM cells. Using primary GBM cells from patients, we demonstrate that allogeneic V γ 9V δ 2 T lymphocytes specifically and spontaneously react against GBM cells with a mesenchymal signature. This work next showed that highly reactive V γ 9V δ 2 T lymphocytes are engaged through both TCR and NKG2D pathways, but independently of a specific TCR signature. Finally, we provided evidence of allogeneic V γ 9V δ 2 T-lymphocyte immunotherapy efficacy *in vivo*, in the absence of any prior sensitization.

Materials and Methods

Human primary GBM cultures

Human primary GBM cultures were obtained after mechanical dissociation of surgical resection tumor samples from patients ($n = 17$). All procedures involving human patients were performed in accordance with the ethical standards of the ethic national research committee and with the 1964 Helsinki declaration and its later amendments or comparable ethical standards. Informed consent was obtained from all individual patients included in this study. Primary cultures were established and stored at -180°C . Cell-frozen vials were grown in defined medium [DMEM/Ham F12 (Gibco), 2 mmol/L L-glutamine (Gibco), N2- and B27-supplement (Gibco), 2 $\mu\text{g}/\text{mL}$ heparin (Sigma Aldrich), 20 ng/mL EGF and 25 ng/mL bFGF (Peprotech), and 100 IU/mL penicillin and 100 mg/mL streptomycin (Gibco)] at 37°C in a humidified atmosphere with 5% CO_2 . All experiments were performed with GBM cells in culture for less than 3 months (passages < 7), and cells were regularly checked for mycoplasma contamination. There are 5 MES cultures (GBM-1, 4, 8, 11, and 12) and 12 CNP (GBM-3, 5, 6, 7, 8, 9, 10, 13, 14, 16, 17, 18, and 19). For pilot studies, GBM-1 and GBM-10 were used as representative of human mesenchymal and CNP tumor cells, respectively.

Generation and expansion of allogeneic human V γ 9V δ 2 T lymphocytes

After informed consent was obtained, human peripheral blood mononuclear cells (PBMCs) were isolated from blood samples of healthy adult volunteers recruited at the Etablissement Français du Sang (EFS). For specific expansions of V γ 9V δ 2 T lymphocytes, PBMC were incubated with 5 $\mu\text{mol}/\text{L}$ of zoledronic acid monohydrate (No. 82712, Sigma-Aldrich) or with 3 $\mu\text{mol}/\text{L}$ of BrHPP (bromohydrin pyrophosphate, kindly provided by Innate Pharma) in RPMI 1640 culture medium supplemented with 10% heat-inactivated FCS, 2 mmol/L L-glutamine, 100 mg/mL streptomycin, 100 IU/mL penicillin (all from Gibco), and 100 IU/mL recombinant human IL2 (rhIL2; Proleukin, Novartis). After 4 days of culture, cells were supplemented with rhIL2 (300 IU/mL). After 3 weeks, a nonspecific expansion was performed using PHA-feeders: Leucoagglutinin PHA-L (No. L4144, Sigma-Aldrich) and 35 Gy-irradiated allogeneic feeder cells mixing human PBMC and Epstein-Barr virus-transformed B-lymphoblastoid cell lines. V γ 9V δ 2 T lymphocytes were incubated in RPMI 1640 culture medium supplemented with 10% heat-inactivated FCS, 2 mmol/L L-glutamine, 100 mg/mL streptomycin, 100 IU/mL penicillin (all from Gibco), and 300 IU/mL rhIL2. After 3 weeks, purity ($>85\%$) of amplified V δ 2⁺ T-lymphocyte cultures was checked by flow cytometry. Clones were obtained by flow cytometry sorting or seeding V γ 9V δ 2 T lymphocytes (0.3 cells/well) in RPMI 1640 medium containing rhIL2,

leukoagglutinin (0.5 mg/mL), and irradiated allogeneic feeder cells (5×10^4 PBL mixed with 5×10^3 transformed human B lymphocytes/well). After expansion, cells were checked for V δ 2 TCR chain expression (purity > 99%) and further expanded using PHA-feeders, as described previously.

Transcriptomic analysis

Primary GBM cells were washed twice in PBS, then total RNA was isolated using the RNeasy MiniKit (Qiagen), according to the manufacturer's instructions with DNase I treatment. The quantity and quality of RNA were, respectively, checked using NanoDrop ND-1000 spectrophotometer (Thermo Fisher Scientific) and Agilent 2100 Bioanalyzer (Agilent). RNA (1.5 mg) was processed and hybridized to the Genechip Human Genome U133 Plus 2.0 Expression array (Affymetrix), which contains over 54,000 probe sets analyzing the expression levels of over 47,000 transcripts and variants. This roughly corresponds to 29,500 distinct Unigene identifiers. The processing was performed according to the recommendations of the manufacturer. The raw signals of each probes for all the arrays were normalized against a virtual median chip (median raw intensity per row) using a local weighted scattered plot smoother analysis. The data were filtered to remove probes with low-intensity values by sample category in order to keep the signature of little class of sample. The hierarchical clustering used to detect groups of correlated genes supported by a statistical method (limma) to detect differential expression among biological conditions was computed on median-gene-centered and log-transformed data using average linkage and uncentered correlation distances with the Cluster program (20). Functional annotations of gene clusters and differential expressed genes were performed using GoMiner software (21) and the Gene Ontology database (22). Raw and normalized data have been deposited in the GEO database under accession number (GSE83626) as previously described in ref. (23). For RNAseq analysis, library construction was performed using 500 ng of total RNA with SureSelect Strand-Specific RNA Library Prep for Illumina Multiplexed kit (5190-6410, Agilent Technologies), according to Agilent_PrepLib_G9691-90010_juillet2015_vD protocol, as described in ref. (24). Purifications were carried out with NucleoMag NGS Clean-up and Size Select (Macherey-Nagel). Fragment size of libraries was controlled on D1000 ScreenTape with 2200 TapeStation system (Agilent Technologies). Libraries with P5-P7 adaptors were specifically quantified on LightCycler 480 Instrument II (Roche Life Science) and normalized with DNA Standards (1-6; No. KK4903, KAPABIOSYSTEMS, Clin-iSciences). Note that 12 pmol/L of each library was pooled and prepared according to denaturing and diluting libraries protocol for the Hiseq and GAlI, part No. 15050107 v02 (Illumina) for cluster generation on cBot™ system. Paired-end sequencing (2×100 cycles) was carried out in four lanes on HiSeq 2500 system (Illumina) in TruSeq v3 chemistry, according to the instructions of HiSeq 2500 System Guide, part No. 15035786 v01 (Illumina). After demultiplexing and quality control with fastQC_0.11.2 (<http://www.bioinformatics.babraham.ac.uk/projects/fastqc/>), Illumina adapter was trimmed with Cutadapt-1.2.1 and reads with Phred quality score below 30 were filtered with prinseq-lite-0.20.3. Reads were aligned against human HG19 reference genome with Tophat2.0.10 and counted with HTseq-count from HTseq-0.5.4p5 and differential analysis with DESeq2.

V γ 9V δ 2 TCR sequencing

Total RNA was purified from indicated V γ 9V δ 2 T-lymphocyte clones using NucleoSpin RNA Plus Kit (Macherey-Nagel), according to the manufacturer's recommendations. Five hundred nanogram RNA was reverse-transcribed using the Maxima First strand cDNA synthesis kit (Thermo Scientific), and cDNA (50 ng) was subsequently amplified using Q5 Hot Start High-Fidelity DNA polymerase and primers targeting variable region of γ (forward 5'-GGTCACCTAGACAACTC-3' and reverse 5'-GTATGTTCCAGCCTTCTGG-3') and δ (forward 5'-GTCATGTCAGCCATTGAG-TTG-3' and reverse 5'-CCTCACCAGACAAGCGAC-3') chains. After checking for single-product amplification on agarose gel, samples were purified using PCR Clean-Up Kit (Macherey-Nagel), according to the manufacturer's recommendations. Purified PCR products were sequenced (Eurofins Genomics). Sequences were analyzed by IMGIT/V-Quest to identify V(D)J segments.

CD107a cell surface mobilization

GBM cells were cocultured with V γ 9V δ 2 T lymphocytes (E:T ratio 1:1) in defined culture medium containing 5 μ mol/L monensin (Sigma-Aldrich) and APC-labeled anti-human CD107a mAb (No. H4A3 from BD Biosciences and BioLegend) for 4 hours at 37°C in a humidified atmosphere with 5% CO₂. V γ 9V δ 2 T lymphocytes were then stained with FITC-labeled anti-human V δ 2 TCR mAb (No. IMMU389; Beckman Coulter) and analyzed by flow cytometry. Acquisition was performed using FACSCalibur or Accuri C6Plus flow cytometer (BD Biosciences), and the events were analyzed using the FlowJo software 10 (Treestar).

Cytolytic activity

Cytolytic activity was assessed through standard ⁵¹Cr -release assays. Primary GBM cultures were labeled with ⁵¹Cr (75 μ Ci for 1×10^6 cells) for 1 hour at 37°C, washed four times with define culture medium, plated at 3×10^3 cells per well, and T lymphocytes were added at the indicated E:T ratios in 96-well round-bottom plates. When indicated, tumor cells were pretreated overnight with zoledronate at 20 mmol/L. For blocking assays, cells were preincubated 30 minutes at 37°C with mouse anti-human CD277/BTN3A1 mAbs (No. 103.2; ImCheck Therapeutics) for primary GBM cultures, and mouse anti-human NKG2D (No. 1D11; BioLegend) for V γ 9V δ 2 T lymphocytes. After a 4-hour coculture at 37°C, ⁵¹Cr released activity was measured in supernatants using a scintillation counter (MicroBeta, Perkin Elmer). Each test was performed in triplicate. Percentage of tumor target cell lysis = [(experimental release-spontaneous release)/(maximum release-spontaneous release)] \times 100. Maximum and spontaneous releases were determined by adding 1% Triton X-100 (Sigma) or medium, respectively, to ⁵¹Cr-labeled tumor target cells in the absence of T lymphocytes.

Cell surface phenotyping

Primary GBM cell surface phenotype was determined by flow cytometry using the following mouse anti-human mAbs: anti-ULBP2, 5, 6-PE (No. 165903), anti-ULBP3-PE (No.166510), anti-ULBP1-AF488 (No. 170818; R&D Systems), anti-MICA/B-PE (No. 6D4; BD Biosciences), and associated isotype controls. To assess the whole NKG2D ligand expression, primary GBM cultures were incubated with FcR-blocking Reagent (Miltenyi Biotec), washed, labeled with 10 μ g/mL recombinant human NKG2D/CD134 Fc Chimera protein (R&D Systems) or isotype control, and incubated with 1 μ g/mL of goat anti-human IgG

Biotin (EFS) followed with Streptavidin-FITC staining (EFS). Vγ9Vδ2 T-cell surface phenotype was determined using anti-human NKG2D-PE (No. ID11; BD Biosciences), anti-NKG2A-PE (No. Z199; Beckman Coulter Immunotech), or corresponding isotype-matched control mAbs. Data were collected using FACS-Calibur (BD Biosciences) cytometer and analyzed using Flowjo 7.6.1 and 8 software (Treestar).

Videomicroscopy

Primary GBM cells were incubated in define medium overnight in Ibidi chamber slides coated with fibronectin (Merck). For intracellular Ca²⁺ measurements, Vγ9Vδ2 T lymphocytes were loaded with 1 mmol/L Fura-2/AM (Invitrogen) in Hank's Balanced Salt Solution (Gibco) supplemented with HEPES (Sigma). Recording was performed using a DMI 6000B microscope (Leica Microsystems). Cells were illuminated every 10 seconds with a 300 W xenon lamp by using 340/10 nm and 380/10 nm excitation filters. Emission at 510 nm was captured using a Cool Snap HQ2

camera (Roper), and ratio measurements were performed with Metafluor software (Molecular Devices).

Stereotactic implantation of GBM cells and transfer of Vγ9Vδ2 T lymphocytes in mice

NSG (*NOD.Cg-Prkdcscid Il2rgtm1Wjl/SzJ*) mice (Charles River Laboratories) mice were bred in the animal facility of the University of Nantes (UTE, SFR F. Bonamy) under specific pathogen-free status and used at 8 to 12 weeks of age, accordingly to institutional guidelines (*Agreement No. 00186.02*; Regional ethics committee of the Pays de la Loire (France)). Primary M1 or CNP1 cultures (1×10^4 in 2-μL PBS) were injected using a stereotactic frame (Stoelting) at 2 mm right lateral of the median suture and 0.5-mm anterior of the Bregma, depth: 2.5 mm. For adoptive T-lymphocyte transfer assays, 2×10^7 allogeneic human Vγ9Vδ2 T lymphocytes in 15- to 20-μL sterile PBS were stereotactically injected into the GBM tumor bed at 7, 14, and 21 days (three injections) after tumor implantation (25).

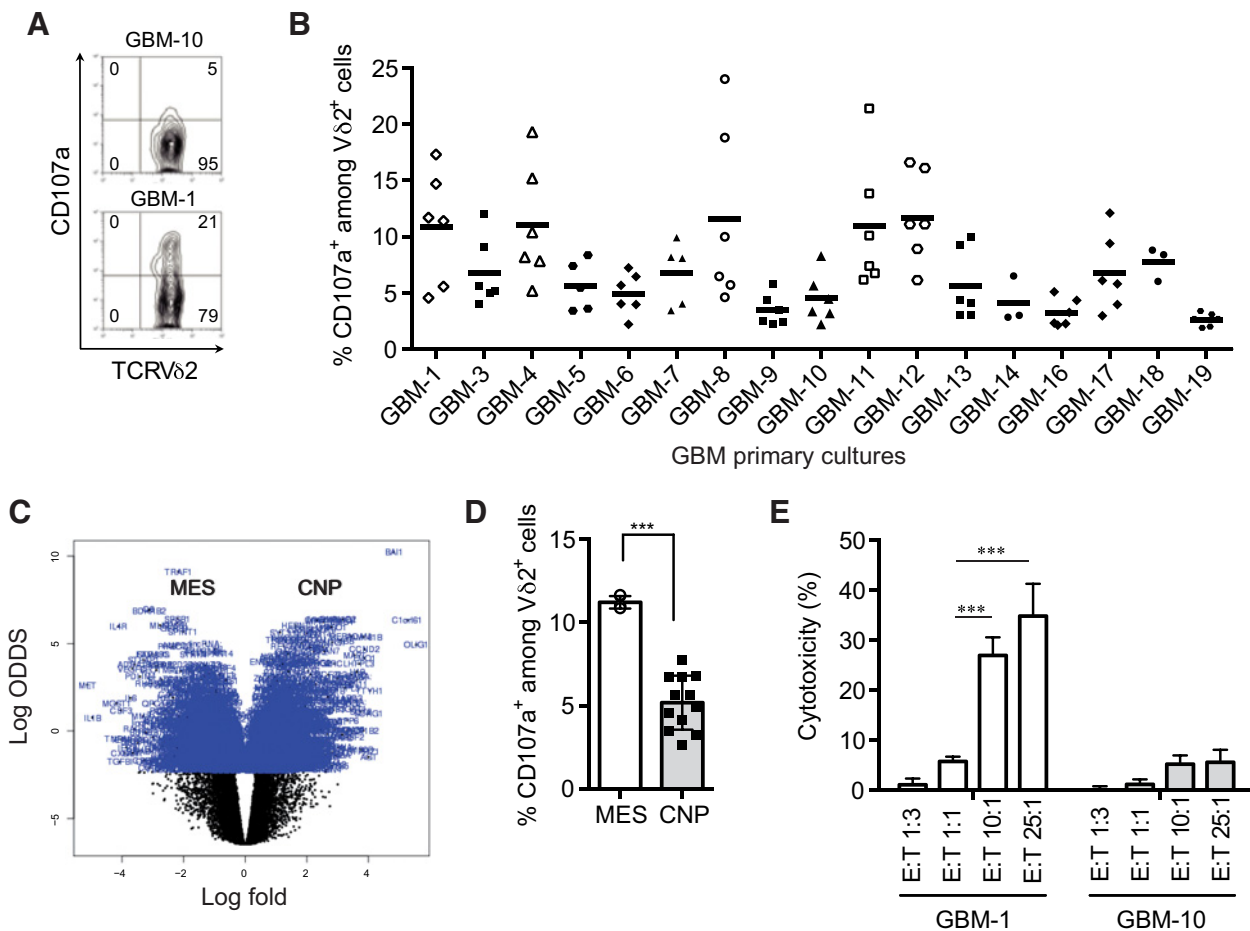


Figure 1. Selective natural cytotoxicity of Vγ9Vδ2 T lymphocytes toward mesenchymal GBM cells. **A**, Representative flow cytometry analysis of CD107a cell surface protein expression of Vγ9Vδ2 T lymphocytes cocultured with primary GBM-1 or GBM-10 cells (E:T ratio 1:1). **B**, Frequency of CD107a⁺ cells among Vγ9Vδ2 T lymphocytes cocultured with 17 primary GBM cultures (E:T ratio 1:1). Each dot represents distinct Vγ9Vδ2 T-cell line. **C**, Volcano plot of CNP vs. MES GBM cells showing the fold ratio and OR. **D**, Mean frequency of CD107a⁺ cells among Vγ9Vδ2 T lymphocytes depending on the molecular subtype of primary GBM cells. Each dot represents distinct primary GBM cells. **E**, Cytotoxicity of Vγ9Vδ2 T lymphocytes against primary GBM cells using ⁵¹Cr-release assays. Results are expressed as percentage of cytotoxicity (mean ± SD, n = 2 in triplicates from two different Vγ9Vδ2 T-lymphocyte lines, Sidak's multiple comparison test; ***, P < 0.001).

Downloaded from <http://aacrjournals.org/clinccancerres/article-pdf/25/23/7218/2055449/7218.pdf> by guest on 13 June 2024

Statistical analysis

Data are expressed as mean ± SD/SEM and were analyzed using GraphPad Prism 6.0 software (GraphPad Software, Inc.). The difference between groups was analyzed by either Sidak, Wilcoxon, ANOVA, Kruskal–Wallis, Mann–Whitney, or log-rank tests (*, $P < 0.05$; **, $P < 0.01$; and ***, $P < 0.001$).

Results

Selective and spontaneous reactivity of allogeneic human Vγ9Vδ2 T lymphocytes against primary mesenchymal human GBM cultures

We previously reported an unexpected spontaneous activation of allogeneic human Vγ9Vδ2 T lymphocytes against some GBM cells as shown in Fig. 1A. We first aimed at extending this observation by analyzing reactivity of peripheral allogeneic human Vγ9Vδ2 T lymphocytes from various healthy donors against a broad panel of primary human GBM cell cultures, directly dissociated from distinct patient tumors ($n = 17$). Of note, primary GBM cultures display single or multiple alterations such as EGFR and/or PDGFR amplification, INK4a/ARF/PTEN loss (Supplementary Table 1). The reactivity of Vγ9Vδ2 T lymphocytes against GBM cells, pretreated or not with NBP, was analyzed after a 4-hour coculture (Fig. 1B; Supplementary Fig. S1A). When primary GBM cells were sensitized with NBP, all Vγ9Vδ2 T lymphocytes strongly upregulated CD107a expression (Supplementary Fig. S1A). Importantly, five of the 17 primary GBM cells spontaneously activated Vγ9Vδ2 T lymphocytes (Fig. 1B). A supervised hierarchical transcriptomic analysis based on the Verhaak transcriptional signatures using our previously published database (GEO GSE83626) identified the spontaneously recognized GBM cells as the mesenchymal subtype and nonnaturally recognized ones as the CNP subtype, as shown in the volcano plot (Fig. 1C). Accordingly, allogeneic Vγ9Vδ2 T lymphocytes reacted stronger against mesenchymal GBM cells

grouped according to this molecular signature, as compared with the other subtypes (Fig. 1D). ⁵¹Cr-release assays were performed using a representative primary GBM cells from either mesenchymal or CNP subtypes, respectively, GBM-1 and GBM-10 cells. As shown in Fig. 1E, Vγ9Vδ2 T lymphocytes spontaneously killed only GBM-1 cells, but not GBM-10 cells, in an E/T-dependent manner. Altogether, these results showed that allogeneic human Vγ9Vδ2 T lymphocytes spontaneously recognize and eliminate mesenchymal human GBM cells, in the absence of any treatment.

Vγ9Vδ2 T lymphocytes display heterogeneous spontaneous reactivity against mesenchymal GBM cells

Besides this selective and spontaneous reactivity against mesenchymal GBM cells, heterogeneous CD107a expression levels observed in activated T lymphocytes also suggested intrinsic activation abilities of Vγ9Vδ2 T lymphocytes. Therefore, we analyzed the reactivity of a panel of allogeneic human Vγ9Vδ2 T lymphocytes ($n = 44$), generated from distinct healthy donor samples, against either GBM-1 or GBM-10 cells. Whereas a weak CD107a expression was detected in the majority of Vγ9Vδ2 T-lymphocyte populations cocultured with GBM-10 cells, this expression level was significantly higher upon coculture with GBM-1 cells (Fig. 2A). Interestingly, this assay identified highly reactive Vγ9Vδ2 T-lymphocyte populations (CD107a-positive cells >20%). Of note, the selective and spontaneous recognition of mesenchymal GBM cells was detected in both highly and poorly reactive Vγ9Vδ2 T-lymphocyte lines (Fig. 2B) and was accompanied by the selective lysis of mesenchymal GBM tumor cells (Fig. 2C). Sensitization of GBM cells with elevated doses of NBP overcame the various levels of reactivity (Supplementary Fig. S1B). These results indicated that, besides their ability to selectively and spontaneously react against mesenchymal GBM cells, allogeneic human Vγ9Vδ2 T-lymphocyte subsets display various functional reactivity abilities toward tumor cells.

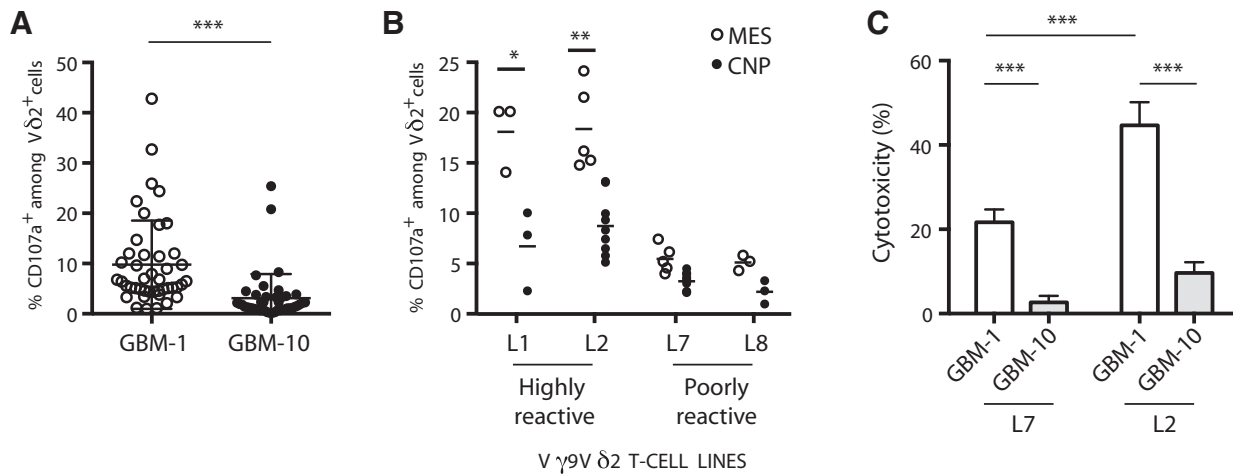


Figure 2. Heterogeneous reactivity of Vγ9Vδ2 T lymphocytes against mesenchymal GBM cells. **A**, Frequency of CD107a⁺ cells among TCRVδ2⁺ lymphocytes (%) after coculture with either the mesenchymal GBM-1 (empty) or CNP GBM-10 (black) cells. Each point corresponds to an individual allogeneic PBMC-derived Vγ9Vδ2 T-lymphocyte lines ($n = 44$, mean ± SD, Wilcoxon matched-pairs signed-rank test: ***, $P < 0.001$). **B**, CD107a expression in four representative Vγ9Vδ2 T-lymphocyte lines after coculture with either mesenchymal (empty spot) or CNP (black spot) GBM cells (two-way ANOVA test: *, $P < 0.05$ and **, $P < 0.01$). **C**, Natural cytotoxicity of two representative Vγ9Vδ2 T-lymphocyte lines (L2 and L7) against either mesenchymal GBM-1 or CNP GBM-10 cells in ⁵¹Cr-release assays (E:T ratio 10:1). Results are expressed as percentage of cytotoxicity ($n = 3$ in triplicates, mean ± SD, two-way ANOVA test: ***, $P < 0.001$).

Downloaded from <http://aacrjournals.org/clinccancerres/article-pdf/25/23/722/18205544/7218.pdf> by guest on 13 June 2024

Vγ9Vδ2 TCR-mediated reactivity is not driven by a specific TCR repertoire

Vγ9Vδ2 TCR contribution was assessed in cytotoxicity assays using BTN3A/CD277-blocking mAb (No. 103.2, Fig. 3A; Supplementary Fig. S1C). To further investigate whether a specific repertoire is linked to this TCR-mediated activation process, T-lymphocyte clones were first isolated from three highly reactive polyclonal Vγ9Vδ2 T-lymphocyte lines with similar natural reactivities (named L1, L2, and L3) from different healthy donors, and next analyzed at transcriptomic/phenotypic (TCR repertoire) and functional (cytotoxicity) levels. Of note, only 25 clones sufficiently expanded among more than hundred clones that emerged in this process. ⁵¹Cr-release assays were performed using mesenchymal GBM-1 cells to determine and compare the relative cytotoxic abilities of each Vγ9Vδ2 T-lymphocyte clones (Fig. 3B). Four clones displayed a cytotoxic activity against GBM-1 cells significantly higher than the polyclonal population, whereas only two clones were significantly less reactive. To next determine whereas such an elevated cytotoxic activity was associated with a specific TCR repertoire, Vγ9 and Vδ2 gene segments were sequenced and analyzed (nomenclature of ref. 26). The majority of clones expressed a similar Vγ9 sequence (TRGV9*01-TRG1P*01), with two clones (No. L3-19, No. L2-9) expressing

different Vγ9 rearrangements (TRGV9*01-TRG1P1*01 and TRGV9*02-TRG1*02, respectively). As expected, more diversity was observed with the Vδ2 TCR repertoire since six signatures were detected. For technical reasons, we could not determine the Vδ2 TCR repertoire for a third of the clones (Fig. 3C, group *nd*). Nevertheless, these results indicated that the Vγ9Vδ2 TCR repertoire was composed of, at least, four distinct clonotypes and that no specific Vγ9Vδ2 TCR signature was assigned to highly reactive T lymphocyte clones (Fig. 3D). Altogether, these results show that selective spontaneous elimination of mesenchymal GBM cells involved TCR engagement, independently of a specific Vγ9Vδ2 TCR repertoire.

Spontaneous elimination of human mesenchymal GBM cells by allogeneic Vγ9Vδ2 T lymphocytes involves NKG2D-activating receptors

In addition to γδ TCR engagement, inhibitory or activating surface molecules are also involved in the reactivity tuning of Vγ9Vδ2 T lymphocytes. Accordingly, single-cell videomicroscopy analyses of early intracellular Ca²⁺ responses in activated Vγ9Vδ2 T lymphocytes showed that cell-to-cell contacts with NBP-sensitized GBM cells triggered rapid and sustained Ca²⁺ responses, characteristic of simultaneous engagement of both

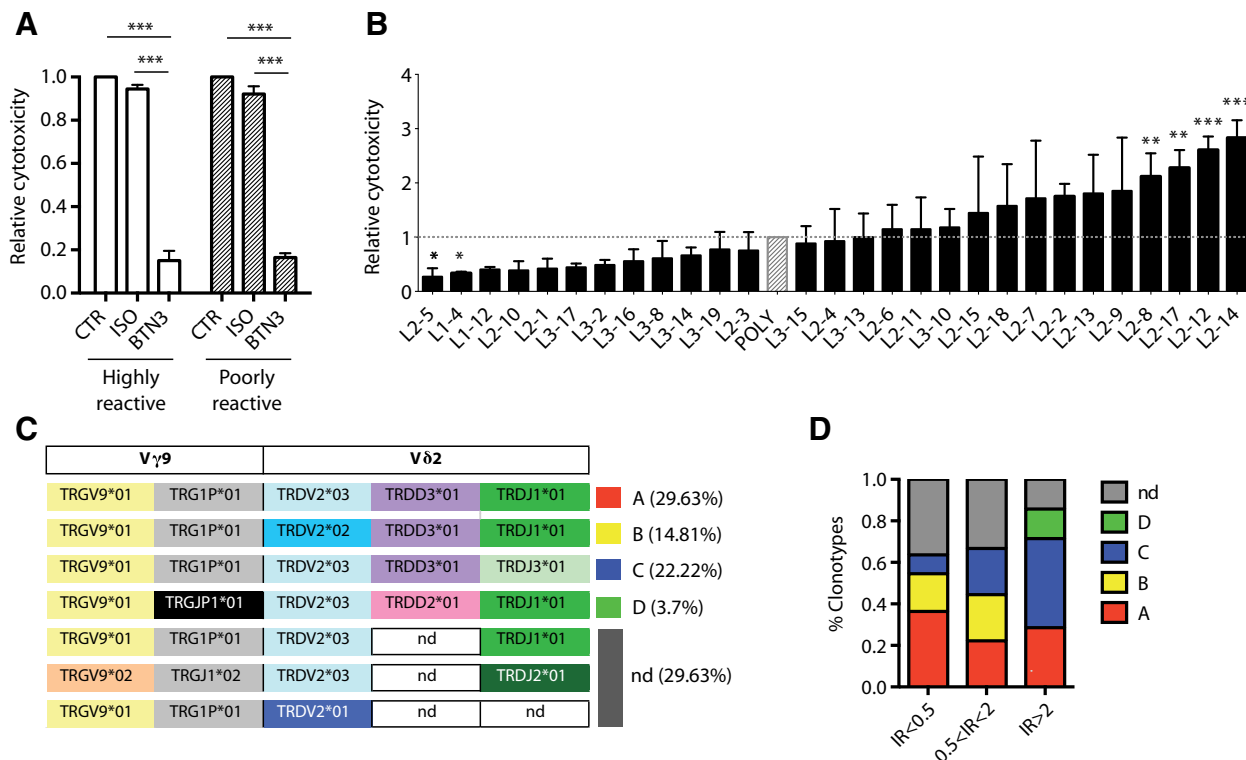


Figure 3. Spontaneous elimination of mesenchymal GBM cells through Vγ9Vδ2 TCR engagement independently of a particular TCR repertoire signature. **A**, Natural cytotoxicity of Vγ9Vδ2 T lymphocytes in the presence of blocking mAb against BTN3A/CD277 (clone No. 103.2). ⁵¹Cr-release assays (E:T ratio 10:1) were performed using either highly or poorly reactive Vγ9Vδ2 T-lymphocyte lines against GBM-1 cells. Relative cytotoxicities of highly (n = 3) and poorly (n = 2) reactive T cells were normalized to cytotoxicity in the absence of blocking antibody (mean ± SD; n ≥ 2 in triplicates, Kruskal-Wallis test: ***, P < 0.001). **B**, Cytotoxicity of Vγ9Vδ2 T-lymphocyte clones generated from three distinct highly reactive Vγ9Vδ2 T-lymphocyte lines (L1, L2, and L3) against GBM-1 cells. Cytotoxicity was analyzed for each clone using ⁵¹Cr-release assays and normalized to respective polyclonal cytotoxicity (E:T ratio: 10:1). Results are expressed as relative cytotoxicity (n = 3 in triplicates, mean ± SD). **C**, TCR repertoires of Vγ9Vδ2 T-lymphocyte clonotypes. Vγ9 and Vδ2 TCR chain sequences are indicated with their respective frequencies among analyzed clonotypes. Undetermined gene segments are indicated as *nd*. **D**, Frequencies of TCR repertoire based on their respective immunoreactivity (IR) profiles.

TCR and receptors interacting with tumor-expressed molecules (Supplementary Fig. S1D). Importantly, in the absence of any NBP sensitization, higher levels of intracellular Ca^{2+} responses were measured in activated $V\gamma 9V\delta 2$ T lymphocytes cocultured with mesenchymal GBM-1 cells, as compared with GBM-10 cells (Fig. 4A). Surface phenotyping of selected activating (DNAM-1, NKG2C, NKG2D, NKP30, NKP44) and inhibitory (NKG2A, ILT2) receptors was performed in various $V\gamma 9V\delta 2$ T-lymphocyte lines. As shown in Fig. 4B, an elevated expression of CD226/DNAM-1 and CD314/NKG2D was detected in all the analyzed lines. Importantly, cytometric analysis showed that NKG2D receptors were expressed at significantly higher levels on mesenchymal GBM-reactive $V\gamma 9V\delta 2$ T lymphocytes, as compared with their poorly reactive lymphocyte counterparts (Fig. 4C). The involvement of NKG2D axis in the spontaneous reactivity was next demonstrated by the results showing the blocking effect of NKG2D mAb (Fig. 4D). The combination of NKG2D and BTN3A (clone No. 103.2) blocking mAbs completely abolished this effect. Of note, NKG2D mAb did not significantly affect the reactivity of $V\gamma 9V\delta 2$ T lymphocytes against GBM cells sensitized

with elevated doses of NBP (Supplementary Fig. S1E). Altogether, these results show that NKG2D, which is highly expressed in GBM-reactive $V\gamma 9V\delta 2$ T lymphocytes, is strongly involved with the TCR in the spontaneous reactivity of allogeneic $V\gamma 9V\delta 2$ T lymphocytes against mesenchymal GBM cells.

Mesenchymal primary GBM cultures express high levels of NKG2D ligands

As spontaneous recognition of human mesenchymal GBM cells by allogeneic $V\gamma 9V\delta 2$ T lymphocytes involves NKG2D receptors expressed by $V\gamma 9V\delta 2$ T lymphocytes, expression profiles of NKG2D ligands in GBM cells were analyzed through transcriptomic and cytometric analyses. Gene analysis using the PANTHER software showed that immune system process, immune response, and response to stress represented three of the six most differentiated pathways between mesenchymal and CNP GBM cells (Fig. 5A). Binding of recombinant human NKG2D Fc chimera protein indicated that NKG2D ligands were expressed at a higher level by mesenchymal GBM cells, as compared with CNP GBM cells (Fig. 5B). Accordingly, levels of RNA encoding for MICA/B

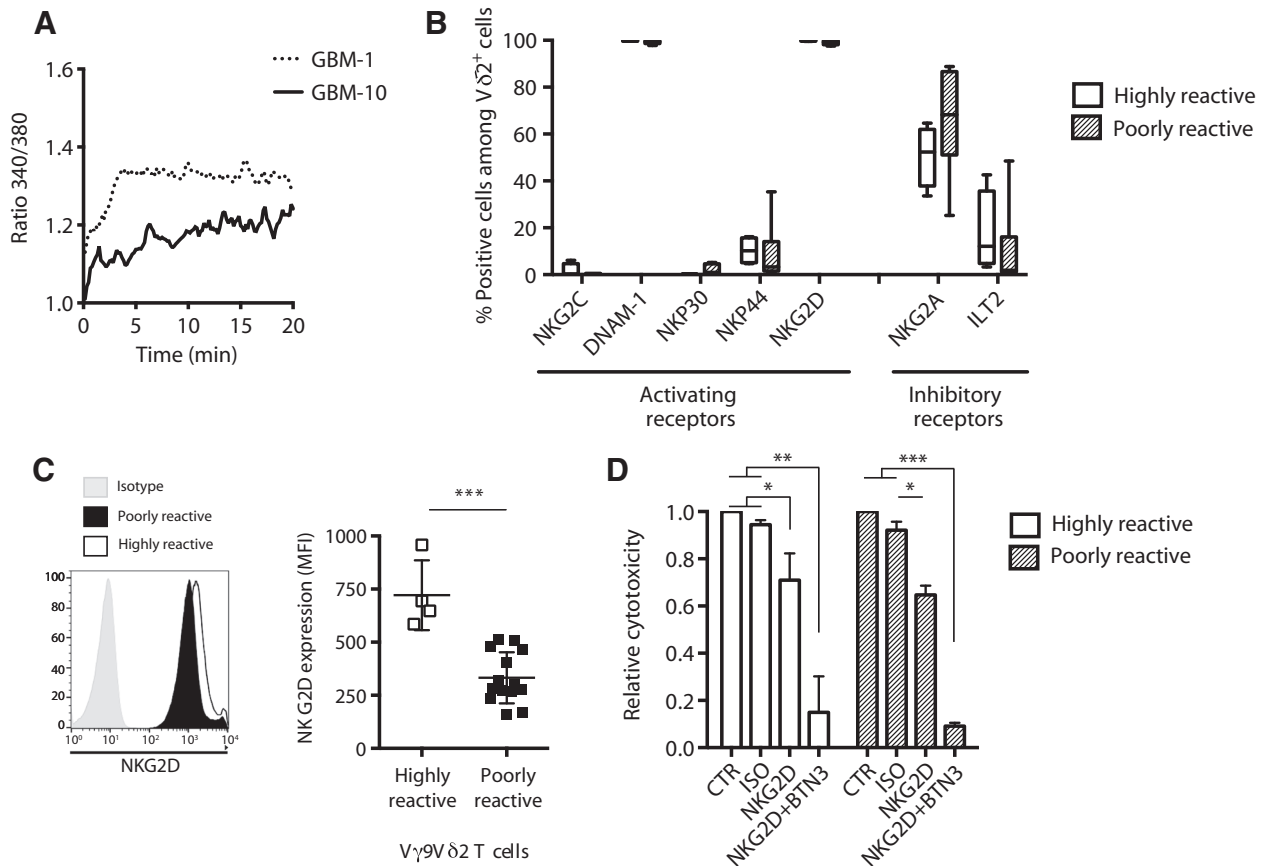


Figure 4. Spontaneous elimination of GBM cells by $V\gamma 9V\delta 2$ T lymphocytes is tuned by NKG2D. **A**, Intracellular Ca^{2+} levels monitored with the Fura-2/AM probe in $V\gamma 9V\delta 2$ T lymphocytes after coculture with either GBM-1 or GBM-10 cells. **B**, Expression of activating and inhibiting NK receptor was analyzed using flow cytometry in highly ($n = 4$) and poorly ($n = 14$) reactive $V\gamma 9V\delta 2$ T-lymphocyte lines. Results are expressed as percentage of positive cells. **C**, Highly ($n = 4$) and poorly ($n = 14$) reactive $V\gamma 9V\delta 2$ T-lymphocyte lines were analyzed by flow cytometry for NKG2D receptor expression. Results are expressed as specific median fluorescence intensity (MFI; MFI isotype control; mean \pm SD; Mann-Whitney test: ***, $P < 0.001$). **D**, Relative cytotoxicity of $V\gamma 9V\delta 2$ T cell against GBM-1 cells (E:T ratio 10:1) in presence of NKG2D-blocking antibody, alone or in combination with BTN3A/CD277-blocking antibody. Relative cytotoxicities of highly ($n = 3$) and poorly ($n = 2$) reactive T cells were normalized to cytotoxicity in absence of blocking antibody (mean \pm SD; $n \geq 2$ in triplicates, Kruskal-Wallis test: *, $P < 0.05$; **, $P < 0.01$; and ***, $P < 0.001$).

Downloaded from <http://aacrjournals.org/clinccancerres/article-pdf/25/23/7218/2055449/7218.pdf> by guest on 13 June 2024

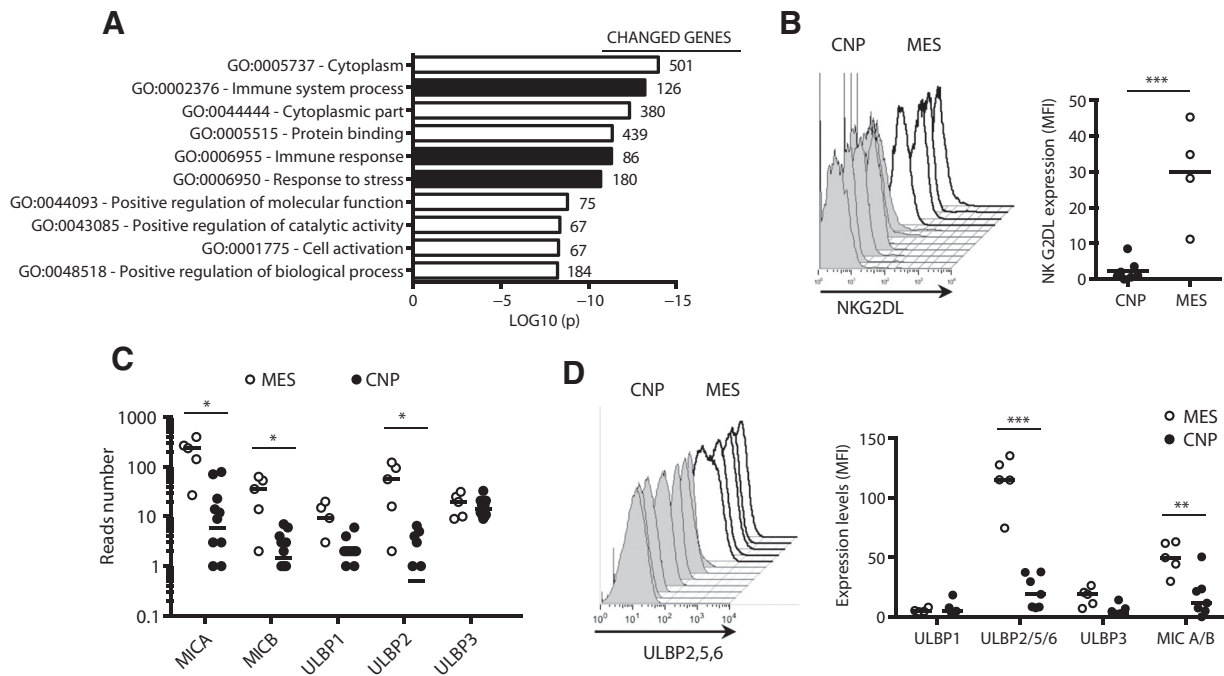


Figure 5. Mesenchymal primary GBM cell cultures highly express NKG2D ligands. **A**, Upregulated pathways in MES primary GBM cultures compared with CNP. Clusters were obtained after transcriptomic analysis followed by functional annotations of differentially expressed genes (GO: Gene Ontology) with indicated number of changed genes. **B**, Tumor cell surface phenotyping performed by flow cytometry with a recombinant human NKG2D-Ig fusion protein to assess whole NKG2D ligands expression. Left, gray and white histograms correspond respectively to CNP and MES GBM cultures. Right, Results are expressed as specific median fluorescence intensity (MFI; mean \pm SD; Mann-Whitney test: ***, $P < 0.001$). **C**, Transcriptomic expression analysis of known Vγ9Vδ2 T-cell ligands in mesenchymal ($n = 5$) and CNP primary cells ($n = 12$). **D**, Tumor cell surface phenotyping was performed by flow cytometry using specific antibodies against ULBP 1, ULBP 2/5/6, ULBP 3, and MIC A/B expression. Histograms correspond to, respectively, CNP and MES GBM cultures as in **B**. Results are expressed as specific median fluorescence intensity (MFI; mean \pm SD; two-way ANOVA test: **, $P < 0.01$ and ***, $P < 0.001$).

(MHC class I Chain related protein A and B) and ULBP2 (UL16 binding protein 2) molecules, which are well-known NKG2D ligands, were detected at significantly higher levels in mesenchymal GBM cultures, as compared with CNP cultures (Fig. 5C). No significant expression of other NKG2D ligands, such as ULBP 4, 5, and 6 molecules, and no significant differential expression for other ligands were detected at the mRNA level (data not shown and Supplementary Fig. S2). Accordingly, expression of ULBP2 and MICA/B proteins was significantly increased at the surface of mesenchymal GBM cells, as compared with CNP cultures (Fig. 5D). These results show that mesenchymal GBM cells highly express several NKG2D ligands, as compared with their CNP counterparts, which might favor their recognition by immune effectors, such as human Vγ9Vδ2 T lymphocytes.

Allogeneic Vγ9Vδ2 T lymphocytes control the development of human mesenchymal GBM tumors *in vivo*

Finally, the ability of Vγ9Vδ2 T lymphocytes to spontaneously control the growth of mesenchymal GBM tumor cells was investigated *in vivo* using preclinical orthotopic mouse models. Human tumor cells from either GBM-1 (mesenchymal) or GBM-10 (CNP) primary cultures were orthotopically implanted into the cerebral subventricular zone of immunodeficient NSG mice. Tumor-bearing mice were then treated with three successive stereotactic injections of allogeneic human Vγ9Vδ2 T lymphocytes performed at days 7, 14, and 21 following tumor implantation (Fig. 6A). As shown in Fig. 6B, untreated GBM-1 tumor-bearing mice

displayed a median survival of 27 days (none, solid line). Three injections of poorly reactive Vγ9Vδ2 T lymphocytes (poorly reactive, dotted line) in GBM-1 mice modestly reduced tumor growth *in vivo*. Strikingly, a clear antitumor activity was measured after three administrations of highly reactive Vγ9Vδ2 T lymphocytes (highly reactive, dashed line). As shown in the table below the survival graph, this latter group could further be divided in poor and good responders with significantly different median survival values of 32 and 58 days, respectively. Importantly, two mice from the good responders group were considered as long-term survivors (>150 days) suggesting a complete elimination of the tumor. Of note, the tumor progression was also delayed in nonmesenchymal GBM-10 tumor-bearing mice after injection of either poorly or highly reactive Vγ9Vδ2 T lymphocytes but to a lesser extent (e.g., absence of long-term survivors; Supplementary Fig. S3). Altogether, these results show that adoptive transfer of allogeneic human PBMC-derived PBL-Vγ9Vδ2 T lymphocytes significantly increased GBM-bearing mouse lifespan, in particular when tumors displayed a mesenchymal signature.

Discussion

This study uncovers an unexpected spontaneous reactivity involving both TCR and NKG2D activating receptors displayed by human Vγ9Vδ2 T lymphocytes against human primary mesenchymal GBM tumor cells.

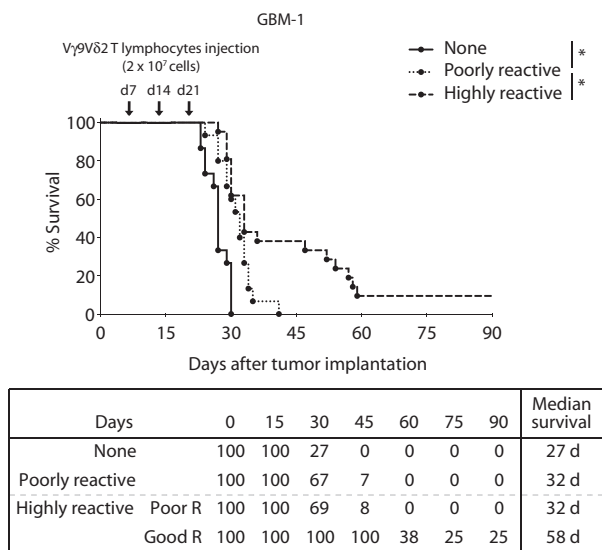


Figure 6. Allogeneic human Vγ9Vδ2 T lymphocytes efficiently eliminate primary mesenchymal GBM cells *in vivo*. Top, Survival curves of GBM-1 tumor-bearing mice untreated (solid line) or treated with poorly (dotted line) or highly (dashed line) reactive Vγ9Vδ2 T lymphocytes. Allogeneic human Vγ9Vδ2 T lymphocytes were injected at the tumor site at days 7, 14, and 21 after tumor cell implantation. Bottom, Relative number of subjects at risk for each group and median survival of GBM-1 tumor-bearing mice treated with Vγ9Vδ2 T lymphocytes are indicated in the table. Mice treated with highly reactive Vγ9Vδ2 T lymphocytes were divided in poor and good responders (R; n = 15 mice treated with poorly or highly reactive Vγ9Vδ2 T lymphocytes, n = 8 for poor responders, and n = 7 for good responders; log-rank test: *, P < 0.05 and ***, P < 0.001).

Human Vγ9Vδ2 T lymphocytes are antigenically activated in a cell-to-cell contact and a TCR-dependent manner. It is currently proposed that nonpeptidic PAg metabolites interact intracellularly with BTN3A1/CD277 butyrophilin molecules, rather than being directly detected by the Vγ9Vδ2 TCR (15, 16), these interactions then specifically trigger T-lymphocyte reactivity. Here, we demonstrated spontaneous recognition of some GBM cells by allogeneic human Vγ9Vδ2 T lymphocytes, in the absence of any NBP sensitization. This process involves Vγ9Vδ2 TCR, as indicated by the results of experiments showing the impact of anti-BTN3A/CD277-blocking mAbs on Vγ9Vδ2 T-lymphocyte activation. Structural diversity of γδ TCR depends on both combinatorial usage of different sets of V, D, and J segments and junctional diversification processes associated with the addition, or loss, of variable numbers of nucleotides at the V-Jγ, V-Dδ, or D-Jδ junctions. In agreement with previous studies showing an intermediate Vγ9Vδ2 V(D)J TCR diversity (reviewed by 27), TCR repertoire analysis of the GBM-reactive T-lymphocyte clones provided evidences for a frequent expression of TCR heterodimers comprising rather conserved recombined Vγ9 chains (mainly TRGV9*01-TRG1P*01 segments), associated to more diverse Vδ2 chains. Importantly, no Vγ9Vδ2 TCR signatures could be specifically assigned to reactive Vγ9Vδ2 T lymphocytes. To illustrate this point, some highly reactive Vγ9Vδ2 T lymphocytes had a Vγ9Vδ2 TCR signature similar to poorly reactive T lymphocytes.

Human Vγ9Vδ2 T lymphocytes sense stress-induced molecules through both TCR and non-TCR molecules (e.g., NK receptors)

that act separately, synergistically, or additively to activate particular T-lymphocyte effector functions through the generation of signals of appropriate strength, duration, and quality (reviewed by 17). In line with previous reports, our study showed that NKG2D homodimers were highly expressed among activating receptors on human Vγ9Vδ2 T lymphocytes and account for this differential reactivity process against human GBM cells. This finding was drawn from a set of complementary observations: (i) the fast kinetics and the intensity of early intracellular Ca²⁺ flux patterns in activated Vγ9Vδ2 T lymphocytes; (ii) the elevated expression levels of several NKG2D ligands in mesenchymal GBM cells, as compared with other GBM subtypes; (iii) the impact of anti-NKG2D-blocking mAbs on Vγ9Vδ2 T lymphocytes reactivity. The importance of this pathway has been previously reported in antitumor reactivities of γδ T lymphocytes in other cancer cells (28). NKG2D ligands have recently been detected in GBM stem cells *in situ* (29) and implicated in the reactivity of Temozolomide-resistant GBM cell lines by Vγ9Vδ2 T lymphocytes (30, 31). Here, we demonstrate for the first time that allogeneic Vγ9Vδ2 T lymphocytes can spontaneously react against human primary GBM cells displaying a mesenchymal signature through high expression of several NKG2D ligands such as ULBP 2 and MICA/B surface stress proteins.

GBM is an archetypical example of heterogeneous cancer with a strong histologic, molecular, and cellular heterogeneity both between patients and within the same individual tumor (6, 32). GBM heterogeneity has been recently extended based on tumor bioenergetic requirements (23). Metabolic changes in tumor cells go beyond the classical tumoral glycolytic avidity. In fact, dysregulation of the mevalonate pathway leading to PAg metabolites accumulation has been reported in tumor cells, including cancer stem cells (33, 34). The ability of human Vγ9Vδ2 T lymphocytes to sense tumor cells has been extensively studied *in vivo* against a variety of tumors, including GBM, in particular after NBP sensitization (19, 25, 35). In this study, we demonstrated a spontaneous recognition of the primary GBM mesenchymal subtype by allogeneic human Vγ9Vδ2 T lymphocytes, in the absence of any NBP sensitization, both *in vitro* and *in vivo*. Whereas bioinformatic analyses did not reveal differences in the expression levels of enzymes of the mevalonate pathway between GBM cell subsets (*data not shown*), using human primary cultures enriched in cancer stem cells, mesenchymal tumor cells clearly exhibit a singular metabolic profile as compared with CNP tumor cells (23). Importantly, in patients, the mesenchymal subtype, representing 30% of *de novo* GBM and 60% of recurrent GBM, has been associated with the worst prognosis (36). In agreement with this dismal prognosis, mesenchymal GBM stem cells are more resistant to radiotherapy and chemotherapy. Thus, the natural and selective eradication of mesenchymal GBM cells, containing highly resistant and infiltrative cancer stem cells, by allogeneic human Vγ9Vδ2 T lymphocytes represents a particularly attractive strategy as the dismal prognosis of GBM is mainly due to tumor recurrence. At the time of recurrence, which usually occurs within the first year of the initial diagnosis, treatment options remain extremely limited, usually depend on medical center expertise as well as patients' individual characteristics, such as age, performance status, tumor location, and time to recurrence, and modestly improve the outcome of the disease (37). Based on our study, we propose stereotactic administrations of allogeneic human PBL-amplified Vγ9Vδ2 T lymphocytes after first-line GBM treatments to specifically track and eliminate mesenchymal GBM tumors, in the absence of NBP

sensitization. Importantly, previous publications have reported that V γ 9V δ 2 T-cell therapy is safe for brain tumor patients (38). Of note, limited brain homing of allogeneic human V γ 9V δ 2 T cells was observed after systemic injections in NSG mice (Jarry U, Joalland N, Scotet E; unpublished data). Furthermore, Halliday and colleagues have shown that radiotherapy promotes a pro-neural–mesenchymal shift (39), in line with increased mesenchymal frequencies in GBM relapse (36). Radiotherapy as well as temozolomide has been shown to increase NKG2D ligand's expression on tumor cells (38, 40). Finally, V γ 9V δ 2 T-lymphocyte reactivity is not restricted by MHC molecules, thus eliminating any risk of deleterious direct alloreactive responses toward nontransformed surrounding cells (38, 41). Therefore, the constitution of selected clinical allogeneic human V γ 9V δ 2 T-lymphocyte banks, established from PBL of healthy donors, would represent a unique opportunity for designing efficient adoptive transfer immunotherapies in patients with GBM.

In this regard, this study highlights novel immunotherapeutic options directed at recurrence of GBM tumors based on adoptive transfer of allogeneic V γ 9V δ 2 T lymphocytes at tumor bed. This work also reinforces molecular subtype identification as a fundamental basis for GBM patient stratification and provides a proof of principle of immunotherapeutic options based on adoptive transfer of allogeneic human V γ 9V δ 2 T lymphocytes, independent of patient immune system status.

Disclosure of Potential Conflicts of Interest

No potential conflicts of interest were disclosed.

Authors' Contributions

Conception and design: C. Chauvin, N. Joalland, U. Jarry, E. Scotet, C. Pecqueur
Development of methodology: C. Chauvin, N. Joalland, X. Saulquin

References

- Stupp R, Mason WP, van den Bent MJ, Weller M, Fisher B, Taphoorn MJB, et al. Radiotherapy plus concomitant and adjuvant temozolomide for glioblastoma. *N Engl J Med* 2005;352:987–96.
- Phillips HS, Kharbanda S, Chen R, Forrest WF, Soriano RH, Wu TD, et al. Molecular subclasses of high-grade glioma predict prognosis, delineate a pattern of disease progression, and resemble stages in neurogenesis. *Cancer Cell* 2006;9:157–73.
- Verhaak RGW, Hoadley KA, Purdom E, Wang V, Qi Y, Wilkerson MD, et al. Integrated genomic analysis identifies clinically relevant subtypes of glioblastoma characterized by abnormalities in PDGFRA, IDH1, EGFR, and NF1. *Cancer Cell* 2010;17:98–110.
- Huse JT, Phillips HS, Brennan CW. Molecular subclassification of diffuse gliomas: seeing order in the chaos. *Glia* 2011;59:1190–9.
- Zheng S, Chheda MC, Verhaak RGW. Studying a complex tumor: potential and pitfalls. *Cancer J Sudbury Mass* 2012;18:107–14.
- Sottoriva A, Spiteri I, Piccirillo SGM, Touloumis A, Collins VP, Marioni JC, et al. Intratumor heterogeneity in human glioblastoma reflects cancer evolutionary dynamics. *Proc Natl Acad Sci U S A* 2013;110:4009–14.
- Patel VN, Gokulrangan G, Chowdhury SA, Chen Y, Sloan AE, Koyutürk M, et al. Network signatures of survival in glioblastoma multiforme. *PLoS Comput Biol* 2013;9:e1003237.
- Brudno JN, Kochenderfer JN. Chimeric antigen receptor T-cell therapies for lymphoma. *Nat Rev Clin Oncol* 2018;15:31–46.
- Herbst RS, Morgensztern D, Boshoff C. The biology and management of non-small cell lung cancer. *Nature* 2018;553:446–54.
- June CH, O'Connor RS, Kawalekar OU, Ghassemi S, Milone MC. CAR T cell immunotherapy for human cancer. *Science* 2018;359:1361–5.
- Wei SC, Duffy CR, Allison JP. Fundamental mechanisms of immune checkpoint blockade therapy. *Cancer Discov* 2018;8:1069–86.
- Lim M, Xia Y, Bettgowda C, Weller M. Current state of immunotherapy for glioblastoma. *Nat Rev Clin Oncol* 2018;15:422–42.
- Silva-Santos B, Serre K, Norell H. $\gamma\delta$ T cells in cancer. *Nat Rev Immunol* 2015;15:683–91.
- Boutin L, Scotet E. Towards deciphering the hidden mechanisms that contribute to the antigenic activation process of human V γ 9V δ 2 T cells. *Front Immunol* 2018;9:828.
- Harly C, Guillaume Y, Nedellec S, Peigné C-M, Mönkkönen H, Mönkkönen J, et al. Key implication of CD277/butyrophilin-3 (BTN3A) in cellular stress sensing by a major human $\gamma\delta$ T-cell subset. *Blood* 2012;120:2269–79.
- Sandstrom A, Peigné C-M, Léger A, Crooks JE, Konczak F, Gesnel M-C, et al. The intracellular B30.2 domain of butyrophilin 3A1 binds phosphoantigens to mediate activation of human V γ 9V δ 2 T cells. *Immunity* 2014;40:490–500.
- Bonneville M, O'Brien RL, Born WK. Gammadelta T cell effector functions: a blend of innate programming and acquired plasticity. *Nat Rev Immunol* 2010;10:467–78.
- Jarry U, Chauvin C, Joalland N, Léger A, Minault S, Robard M, et al. Stereotoxic administrations of allogeneic human V γ 9V δ 2 T cells efficiently control the development of human glioblastoma brain tumors. *Oncoimmunology* 2016;5:e1168554.
- Joalland N, Chauvin C, Oliver L, Vallette FM, Pecqueur C, Jarry U, et al. IL-21 increases the reactivity of allogeneic human V γ 9V δ 2 T cells against primary glioblastoma tumors. *J Immunother Hagerstown Md* 1997 2018;41:224–31.
- de Hoon MJL, Imoto S, Nolan J, Miyano S. Open source clustering software. *Bioinforma Oxf Engl* 2004;20:1453–4.
- Zeeberg BR, Feng W, Wang G, Wang MD, Fojo AT, Sunshine M, et al. GoMiner: a resource for biological interpretation of genomic and proteomic data. *Genome Biol* 2003;4:R28.

Acquisition of data (provided animals, acquired and managed patients, provided facilities, etc.): C. Chauvin, N. Joalland, J. Perroteau, U. Jarry, C. Retière, L. Oliver, C. Gratas

Analysis and interpretation of data (e.g., statistical analysis, biostatistics, computational analysis): C. Chauvin, N. Joalland, J. Perroteau, U. Jarry, C. Willem, C. Retière, L. Gautreau-Rolland, H. Vié, C. Pecqueur

Writing, review, and/or revision of the manuscript: C. Chauvin, N. Joalland, C. Gratas, X. Saulquin, H. Vié, E. Scotet, C. Pecqueur

Administrative, technical, or material support (i.e., reporting or organizing data, constructing databases): C. Chauvin, N. Joalland, L. Lafrance, F.M. Vallette

Study supervision: E. Scotet, C. Pecqueur

Acknowledgments

We thank the Cytocell, MicroPicell, and UTE facilities (SFR. F. Bonamy, Université de Nantes, France) and staff for technical help. We would like to thank Sylvia Lambot, Pierre Autin, Lucie Lebreuilly, and Fanny Geraldo for technical help. We would like to thank Dr. Richard Hellman for proofreading the article.

This work was supported by INSERM, CNRS, Université de Nantes, Association pour la Recherche contre le Cancer, Institut National du Cancer (INCa#PL-Bio2013-201, #PLBio2014-155), Ligue Nationale contre le Cancer. This work was realized in the context of the LabEX IGO and the IHU-Cesti programs, supported by the National Research Agency Investissements d'Avenir via the programs ANR-11-LABX-0016-01 and ANR-10-IBHU-005, respectively. The IHU-Cesti project is also supported by Nantes Metropole and the Pays de la Loire Region.

The costs of publication of this article were defrayed in part by the payment of page charges. This article must therefore be hereby marked *advertisement* in accordance with 18 U.S.C. Section 1734 solely to indicate this fact.

Received February 13, 2019; revised May 28, 2019; accepted August 29, 2019; published first September 10, 2019.

22. Ashburner M, Ball CA, Blake JA, Botstein D, Butler H, Cherry JM, et al. Gene ontology: tool for the unification of biology. The Gene Ontology Consortium. *Nat Genet* 2000;25:25–9.
23. Oizel K, Chauvin C, Oliver L, Gratas C, Geraldo F, Jarry U, et al. Efficient mitochondrial glutamine targeting prevails over glioblastoma metabolic plasticity. *Clin Cancer Res* 2017;23:6292–304.
24. Leveque X, Hochane M, Geraldo F, Dumont S, Gratas C, Oliver L, et al. Low-dose pesticide mixture induces accelerated mesenchymal stem cell aging in vitro. *Stem Cells* 2019;37:1083–94.
25. Jarry U, Joalland N, Chauvin C, Clemenceau B, Pecqueur C, Scotet E. Stereotactic adoptive transfer of cytotoxic immune cells in murine models of orthotopic human glioblastoma multiforme xenografts. *J Vis Exp JoVE* 2018;139:e57870.
26. Lefranc MP, Rabbitts TH. A nomenclature to fit the organization of the human T-cell receptor gamma and delta genes. *Res Immunol* 1990;141:615–8.
27. Hoeres T, Smetak M, Pretscher D, Wilhelm M. Improving the efficiency of V γ 9V δ 2 T-cell immunotherapy in cancer. *Front Immunol* 2018;9:800.
28. Wrobel P, Shojaei H, Schittek B, Gieseler F, Wollenberg B, Kalthoff H, et al. Lysis of a broad range of epithelial tumour cells by human gamma delta T cells: involvement of NKG2D ligands and T-cell receptor- versus NKG2D-dependent recognition. *Scand J Immunol* 2007;66:320–8.
29. Flüh C, Chitadze G, Adamski V, Hattermann K, Synowitz M, Kabelitz D, et al. NKG2D ligands in glioma stem-like cells: expression in situ and in vitro. *Histochem Cell Biol* 2018;149:219–33.
30. Chitadze G, Lettau M, Luecke S, Wang T, Janssen O, Fürst D, et al. NKG2D- and T-cell receptor-dependent lysis of malignant glioma cell lines by human $\gamma\delta$ T cells: Modulation by temozolomide and A disintegrin and metalloproteases 10 and 17 inhibitors. *Oncoimmunology* 2015;5:e1093276.
31. Lamb LS, Bowersock J, Dasgupta A, Gillespie GY, Su Y, Johnson A, et al. Engineered drug resistant $\gamma\delta$ T cells kill glioblastoma cell lines during a chemotherapy challenge: a strategy for combining chemo- and immunotherapy. *PLoS One* 2013;8:e51805.
32. Patel M, Vogelbaum MA, Barnett GH, Jalali R, Ahluwalia MS. Molecular targeted therapy in recurrent glioblastoma: current challenges and future directions. *Expert Opin Investig Drugs* 2012;21:1247–66.
33. Ginestier C, Monville F, Wicinski J, Cabaud O, Cervera N, Josselin E, et al. Mevalonate metabolism regulates Basal breast cancer stem cells and is a potential therapeutic target. *Stem Cells* 2012;30:1327–37.
34. Gober H-J, Kistowska M, Angman L, Jenö P, Mori L, De Libero G. Human T cell receptor gammadelta cells recognize endogenous mevalonate metabolites in tumor cells. *J Exp Med* 2003;197:163–8.
35. Fisher JP, Heuwerkerk J, Yan M, Gustafsson K, Anderson J. $\gamma\delta$ T cells for cancer immunotherapy: a systematic review of clinical trials. *Oncoimmunology* 2014;3:e27572.
36. Wang Q, Hu B, Hu X, Kim H, Squatrito M, Scarpace L, et al. Tumor evolution of glioma intrinsic gene expression subtype associates with immunological changes in the microenvironment. *Cancer Cell* 2017;32:42–56.e6.
37. van Linde ME, Brahm CG, de Witt Hamer PC, Reijneveld JC, Bruynzeel AME, Vandertop WP, et al. Treatment outcome of patients with recurrent glioblastoma multiforme: a retrospective multicenter analysis. *J Neurooncol* 2017;135:183–92.
38. Pereboeva L, Harkins L, Wong S, Lamb LS. The safety of allogeneic innate lymphocyte therapy for glioma patients with prior cranial irradiation. *Cancer Immunol Immunother* 2015;64:551–62.
39. Halliday J, Helmy K, Pattwell SS, Pitter KL, LaPlant Q, Ozawa T, et al. In vivo radiation response of proneural glioma characterized by protective p53 transcriptional program and proneural-mesenchymal shift. *Proc Natl Acad Sci U S A* 2014;111:5248–53.
40. Weiss T, Schneider H, Silginer M, Steinle A, Pruschy M, Polić B, et al. NKG2D-dependent antitumor effects of chemotherapy and radiotherapy against glioblastoma. *Clin Cancer Res* 2018;24:882–95.
41. Lamb LS, Musk P, Ye Z, van Rhee F, Geier SS, Tong JJ, et al. Human gammadelta(+) T lymphocytes have in vitro graft vs leukemia activity in the absence of an allogeneic response. *Bone Marrow Transplant* 2001;27:601–6.